JOURNAL OF MATERIALS SCIENCE 15 (1980) 939–944

An electron beam induced current study of grain boundaries in zinc selenide

G. J. RUSSELL, M. J. ROBERTSON, B. VINCENT, J. WOODS
Department of Applied Physics and Electronics, University of Durham, South Road, Durham DH1 3LE, UK

An electron beam induced current investigation of crystalline samples of zinc selenide in the scanning electron microscope has proved particularly useful in revealing the existence of grain boundaries. Changes in the EBIC contrast which are observed when the bias is altered, or at places where twin bands intersect the grain boundaries, are explained in terms of a model which associates a potential energy barrier, similar to two Schottky barriers back to back, with a grain boundary.

1. Introduction

Although the electron beam induced current (EBIC) mode of operation of the scanning electron microscope (SEM) has been used for several years to study such crystalline defects as dislocations [1] and stacking faults [2], there is little recorded evidence so far of its use in the examination of grain boundaries [3]. However, we have found the method to be of great assistance in studying grain boundaries in single crystals of ZnSe doped with indium or gallium. Such material is particularly well suited to EBIC investigation since its resistivity can be varied over a wide range from 10 to $10^7\ \Omega$ cm, or larger, by altering the doping concentration. The purpose of this paper is to describe the nature of the EBIC contrast produced at grain boundaries, and to offer an explanation of the various features observed.

The electrical properties of ZnSe doped with indium or gallium are interesting because unusual donor compensation effects occur at increasing concentrations of the added impurity [4, 5]. Indeed, there are reports [6], that heavily doped epitaxial layers of ZnSe : In have been made *p*-type. We, in this laboratory, have been studying the electrical properties of ZnSe:In and ZnSe:Ga for some time past, and for this purpose have usually prepared samples in the form of small bars (8 mm × 2 mm × 1 mm), with indium contacts at either end, and at intervals along the length. It is quite evident that an applied voltage is not always dropped uniformly along the length of a sample, and such non-uniformity is usually found to have been caused by the potential barrier provided by a grain boundary. Such samples are unsuitable for the evaluation of electrical properties, but are eminently suitable for the investigation of grain boundaries in the EBIC mode in the SEM.

2. Experimental procedure

The crystals for this work were grown using the vapour phase technique described by Cutter *et al.* [7], with the modification that appropriate quantities or indium or indium doped ZnSe were added to the charge to produce boules containing concentrations of indium in the range 5 to 1000 p.p.m. Actual indium concentrations were determined by atomic absorption spectroscopy. Undoped crystals of ZnSe were also used in control experiments, but it was necessary first to heat them in molten zinc at 850° C for 48 h to reduce their resistivities from about $10^{12}\ \Omega$ cm to about $10\ \Omega$ cm.

The bars with dimensions of 8 mm × 2 mm × 1 mm were cut from the boules using a diamond wheel. The faces of the bars were mechanically polished with 1 μm diamond paste and were then chemically etched in a 1% solution of bromine in methanol. After the samples had been rinsed successively in methanol, carbon disulphide and absolute alcohol, contacts were applied by pressing pellets of indium on to them. Finally the bars were heated in argon for 10 min at 300° C.

0022–2461/80/040939–06$02.60/0

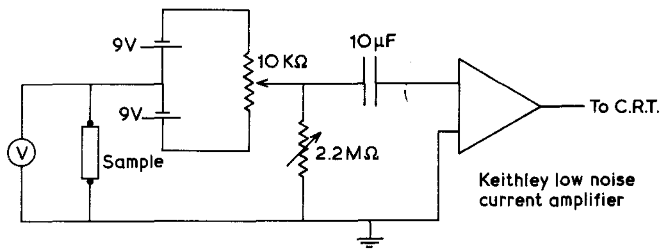

Figure 1 Biassing and EBIC signal detection circuit for high impedance samples.

The specimens were examined in a Cambridge S600 SEM employing a Keithley specimen current amplifier type 427 to produce the EBIC images. A biassing arrangement was incorporated in the amplifier circuit, see Fig. 1, to enable the behaviour of electrically active defects to be studied as a function of bias voltage.

3. Experimental observations

When the indium-doped specimens which exhibited a non-uniform distribution of potential were examined using the EBIC technique, contrast was immediately apparent at some of the grain boundaries, see Fig. 2. This contrast is similar to that produced by the barrier electron voltaic effect at p–n junctions in semiconductors [8]. However it differed from the latter effect in that it changed from white (Fig. 2) to black (Fig. 3), when the potential applied to one of the end contacts was changed from + 3 V to − 3 V relative to the other. Fig. 4 is the secondary emission micrograph of the same region of the sample. The grain boundary which gave rise to the EBIC contrast is clearly visible. The lines of light contrast which do not deviate as they cross the grain boundary are associated with saw marks from the diamond wheel which were not removed by the mechanical and chemical polishing from this particular sample. The abrupt termination of twin bands at B draws attention to another grain

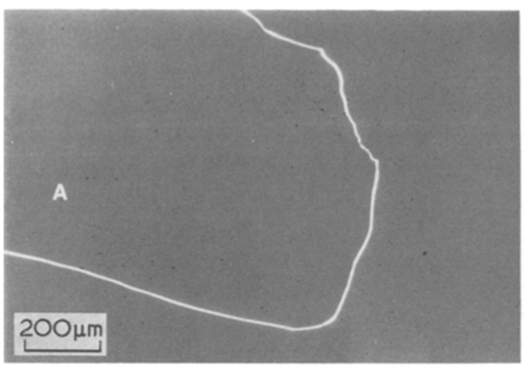

Figure 2 EBIC micrograph of a grain boundary in ZnSe where + 3 V is applied to grain A.

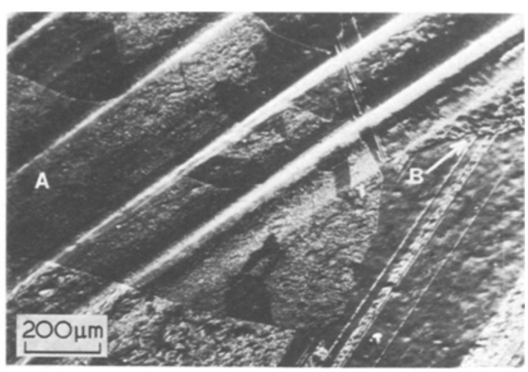

Figure 4 Secondary emission micrograph of the region shown in Fig. 2 with no bias.

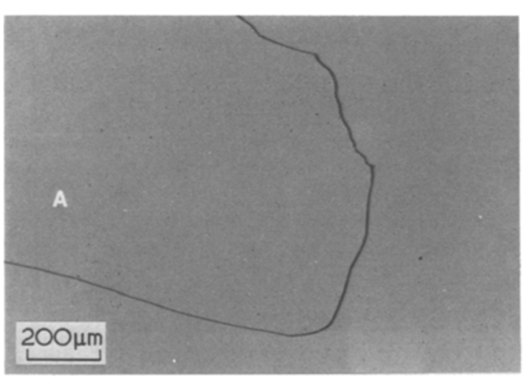

Figure 3 EBIC micrograph of the region shown in Fig. 2 where − 3 V is applied to grain A.

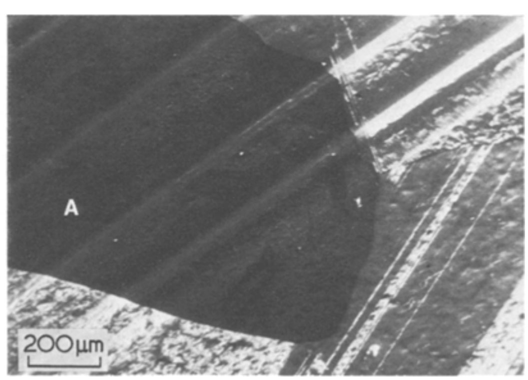

Figure 5 Secondary emission micrograph of the region shown in Fig. 2 where + 3 V is applied to grain A.

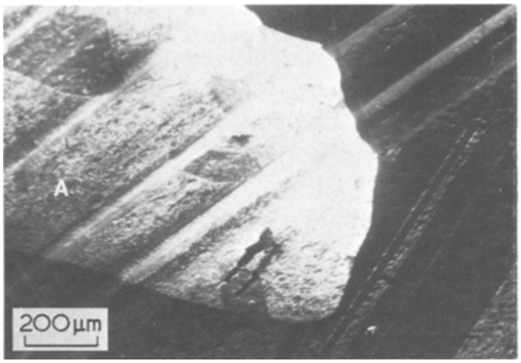

Figure 6 Secondary emission micrograph of the region shown in Fig. 2 where − 3 V is applied to grain A.

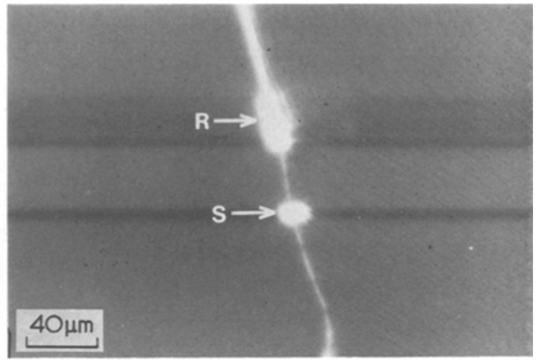

Figure 7 Micrograph showing the modification to the EBIC signal where twin bands meet a grain boundary in ZnSe.

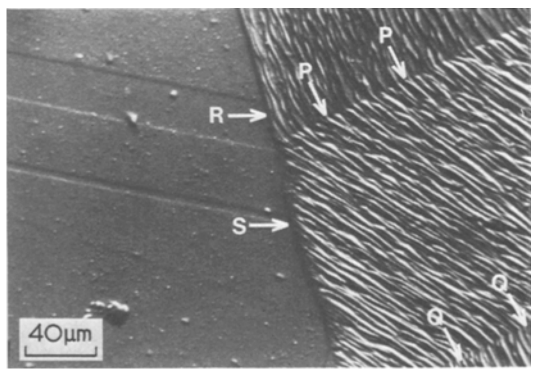

Figure 8 Secondary emission micrographs of the region shown in Fig. 7.

boundary, which, with the electrode configuration employed, was not active in the EBIC mode. However, contrast at this grain boundary was readily obtainable when the bias was applied to a different set of electrodes. In general the boundaries active in the EBIC mode formed a single continuous barrier between the two electrodes across which the potential was applied. Boundaries connecting the two electrodes were invariably inactive in the EBIC mode.

Confirmation that the EBIC contrast shown in Figs. 2 and 3 was associated with an electrical barrier along a grain boundary was provided by the voltage contrast effects observed in secondary emission. Figs. 5 and 6 show secondary emission micrographs of the same area seen in Fig. 4. Fig. 4 was obtained with zero voltage applied to the sample, but Figs. 5 and 6 resulted when the grain A was biassed to + 3 V and − 3 V relative to the remainder of the sample. In both the latter two micrographs the contrast is uniform in two separate regions, inside or outside of grain A. In each micrograph the region of light contrast corresponds to a surface carrying a negative potential, while the area of dark contrast corresponds to regions with a positive one. Thus an abrupt potential difference occurs only at the boundary which surrounds grain A. It is interesting to record that when the bias was increased to about 30 V, so that a current density of some 5 A cm^{-2} was flowing, spots of yellow light were emitted from the same grain boundary surrounding grain A. This light emission is no doubt associated with regions of high localized electric field.

An important feature of the EBIC signal emanating from grain boundaries was its dependence of the local crystallography. This was most obvious at places where twin bands terminated at an electrically active boundary thus introducing local modifications in the crystal structure at the intersection of the two grains. An example illustrating this effect is shown in Fig. 7, while the corresponding secondary emission micrograph forms Fig. 8. Comparison of the two micrographs reveals that the two twin bands in the grain on the left-hand side in Fig. 8, give rise to a broadening of the EBIC signal at points R and S on the boundary, as is clearly evident in Fig. 7. From a closer inspection of Fig. 8 the presence of twin boundaries can also be inferred along PP and QQ where the striations produced by the etching change direction. The presence of this wide twin band on the right-hand side of Fig. 8 gives rise to an EBIC signal which is broader at the top of Fig. 7 than that at the bottom.

The effect of reversing the polarity of the voltage applied to the region shown in Fig. 7 is recorded in Fig. 9. Comparison of the two EBIC images leads to the conclusion that EBIC signals that are wide for one sign of applied voltage are

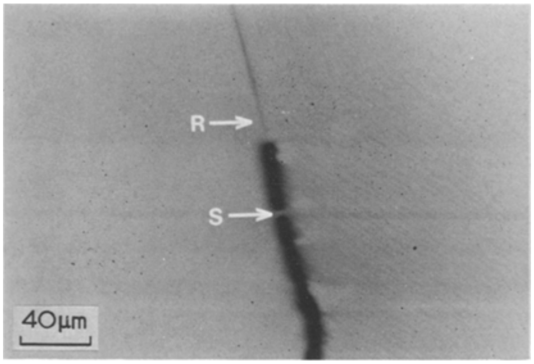

Figure 9 EBIC micrograph of the region shown in Fig. 7 with the polarity of the applied voltage reversed.

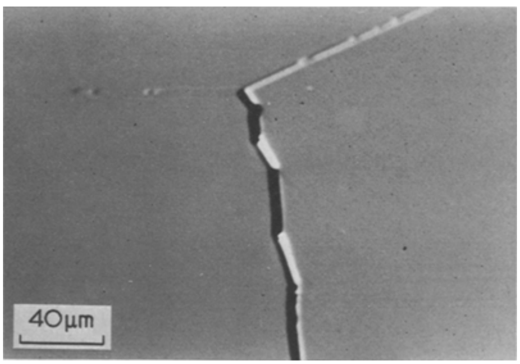

Figure 10 EBIC micrograph from another grain boundary in ZnSe with zero applied bias.

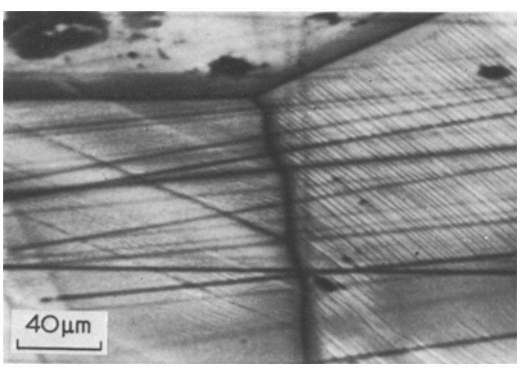

Figure 11 Cathodoluminescent image of the region shown in Fig. 10.

narrow for the other, and vice versa. An interesting consequence of this effect is the form of the EBIC signal obtained with zero bias. Such an image is shown in Fig. 10, which is from a different area from that used to obtain Figs. 7 and 9. It does however correspond to a grain boundary with twin bands terminating along its length. The zero bias contrast takes a form which is intermediate between those exhibited by a similar boundary in the two different bias conditions shown in Figs. 7 and 9. The grain boundary then gives rise to a black/white contrast to varying degrees along its length. By rotating the sample through 180° in the SEM it was demonstrated that this particular contrast was independent of the direction of the beam scan. The origin of the contrast effect is discussed below.

Finally, it is worth mentioning that examination of the samples in the SEM in the cathodoluminescence mode shows that the luminescence was always suppressed at the grain boundaries. This is illustrated in Fig. 11 which is a cathodoluminescent image of the same area which provided the EBIC image shown in Fig. 10. Clearly radiationless recombination occurs preferentially at these grain boundaries.

4. Discussion

The qualitative model proposed to explain the EBIC observations can be understood by reference to the potential energy diagrams shown in Fig. 12. At some grain boundaries the conduction and valence bands of the *n*-type ZnSe will be bent upwards as illustrated in Fig. 12a. The band bending may well be a consequence of the segregation of impurities to the grain boundaries where they can act as acceptor states. Electrons from donors in the immediate vicinity would be captured by the acceptors, producing a layer of negative charge at the grain boundary, and leaving a region of positive space charge in the ZnSe close to the boundary. The width of the resultant depletion region would depend on the conductivity of the grain and the concentration of surface acceptor states at the grain boundary. The suggestion is therefore that each grain boundary would be accompanied by a potential barrier similar to that in Fig. 12a, and consequently each grain boundary would have a built-in electric field associated with it. When such grain boundaries with their associated depletion regions form a continuous barrier between contacts, they will limit the total current flow. Electron bombardment within a depletion region will then lead to a beam induced current so that contrast will be observed in the EBIC mode. When a grain boundary forms a connecting path between the contacts, the accompanying depletion regions will have a very small effect on the total current flow, with the result that

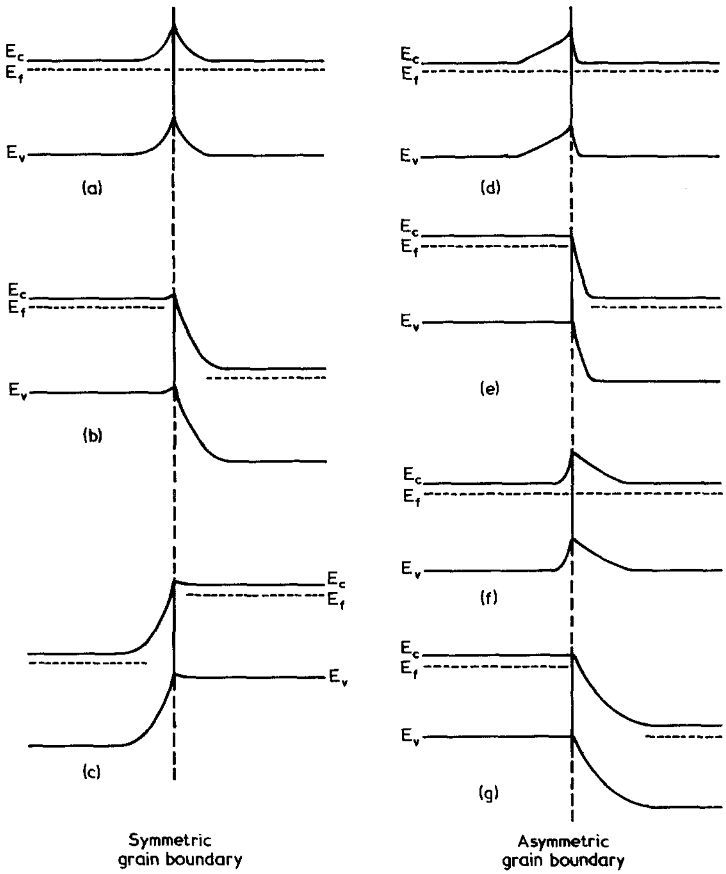

Figure 12 Energy band diagrams for: (a) a symmetric grain boundary without bias. (b) The boundary in (a) with negative bias on the left-hand side. (c) The boundary in (a) with negative bias on the right-hand side. (d) An asymmetric grain boundary without bias. (e) The boundary in (d) with negative bias on the left-hand side. (f) The other configuration for an asymmetric grain boundary without bias. (g) The boundary in (f) with negative bias on the left-hand side.

bombardment within the depletion region will have virtually no effect on the total current flow. No EBIC contrast therefore will be observed.

Consider next what happens when the electron beam is scanned from left to right across a grain boundary with an associated potential barrier such as that depicted in Fig. 12a. Assume first that zero bias is applied. When the beam reaches the left-hand depletion region, the beam-induced electron–hole pairs are separated by the internal field, and the majority carriers (electrons) are swept towards the left-hand contact while the minority carriers (holes) recombine via the recombination centres at the grain boundary with electrons captured from either side of the boundary. That such recombination centres exist is demonstrated by the cathodoluminescent image in Fig. 11 which shows that luminescence is suppressed at grain boundaries. If the sample is connected so that the electron current flow to the left from the grain boundary produces a dark image on the screen, then a black line will be formed just to the left of the grain boundary. When the beam reaches the right-hand side of the grain-boundary, the current flowing in the external circuit will reverse and electrons will flow from left to right. A white line will then be produced in the EBIC image. This is exactly what is observed in Fig. 10.

When a bias is applied to the sample, the potential energy barriers become asymmetric as shown in Figs. 12b and c, which are for the two possible polarities of the applied voltage. As the beam scans a biassed barrier, Fig. 12b, little separation of the induced electron–hole pairs to the left of the barrier occurs, so that the total current is only slightly affected. On the right-hand side of the barrier, however, a high field exists so that the electron–hole pairs are readily swept apart. As a result an intense white line appears in the EBIC image as in Fig. 2. With reversed polarity the potential energy diagram in Fig. 12c is appropriate and clearly the beam induced electron current now flows from right to left, producing a dark line in the EBIC mode, Fig. 3. In effect, if the barriers in Figs. 12b and c are regarded as two Schottky barriers back-to-back, one of the Schottky barriers is biassed in the forward direction and the other in the reverse. A beam induced current would only be expected at a reverse-biassed Schottky barrier. In this discussion of the contrast when an external voltage is applied, it has been assumed that virtually all the voltage is dropped across the grain boundary. This is indeed a reasonable assumption as the micrographs obtained in secondary emission with voltage contrast (Figs. 5 and 6) show.

The more complicated EBIC effects illustrated in Figs. 7 and 9 can be explained if the extent of the band bending is different on either side of the grain boundary, as in Figs. 12d and f, and varies when the crystallographic orientation of the grains changes (for example when twin bands intersect the grain boundary). The different widths of the black and white portions of the unbiassed EBIC images in Fig. 10 can also be explained with the same model, namely that a barrier such as that in Fig. 12d will have a broader stripe of contrast on the left corresponding to the wider depletion region.

With the appropriate bias applied, the barrier in Fig. 12d goes over to that in Fig. 12e, while 12f goes to 12g. In Fig. 12e the internal field is large and the depletion region is relatively narrow; as a result the white line in the EBIC image, is narrow as can be seen in the bottom half of Fig. 7. With the situation shown in Fig. 12g however, the electric field extends over a wider region, leading to the broader white region at the top of Fig. 7. When the bias is reversed, Fig. 12e, for example, will be replaced with a diagram in which the space charge region now on the left of the barrier is wider than that on the right in Fig. 12e. This means that reversal of polarity will lead to the replacement of a narrow white stripe with a broad black one; a narrow black line will also replace a broad white one. This is clearly shown in Fig. 9.

In conclusion, it might be remarked that the EBIC technique has proved to be invaluable in demonstrating which samples of ZnSe are most useful for the evaluation of the electrical properties of the material, i.e. to demonstrate which samples contain no potential barriers and which can therefore be used to provide meaningful Hall coefficient measurements, etc. The proposed qualitative theory of grain boundary barriers can explain all the observed phenomena and could, if necessary, be put on a quantitative basis. Preliminary attempts to determine whether segregation of indium to the grain boundaries is primarily responsible for the band bending have proved inconclusive, but it should be reported that we have also observed similar EBIC contrast effects at grain boundaries in nominally undoped samples of ZnSe that have been heat treated in molten Zn at 850° C.

References

1. W. CZAJA and J. R. PATEL, *J. Appl. Phys.* **36** (1965) 1476.
2. T. E. SEIDEL, S. E. HASZKO and D. M. MAHER, *ibid.* **48** (1977) 5038.
3. C. MUNAKATA, *Japan J. Appl. Phys.* **5** (1966) 1251.
4. G. JONES and J. WOODS, *J. Phys. D (Appl. Phys.)* 9 (1976) 799.
5. B. R. SETHI, P. C. MATHUR and J. WOODS, *J. Appl. Phys.* **50** (1979) 352.
6. Z. K. KUN and R. J. ROBINSON, *J. Electron. Mater.* **5** (1976) 23.
7. J. R. CUTTER, G. J. RUSSELL and J. WOODS, *J. Cryst. Growth* **32** (1976) 179.
8. D. B. HOLT, B. D. CHASE and M. CENSLIVE, *Phys. Stat. Sol. a* **20** (1973) 459.

Received 3 August and accepted 20 September 1979.